A PATH-FOLLOWING PREVIEW CONTROLLER FOR AUTONOMOUS UNDERWATER VEHICLES[1]

Nuno Paulino Carlos Silvestre * **Rita Cunha** *
António Pascoal *

* *Instituto Superior Técnico, Institute for Systems and Robotics*
Av. Rovisco Pais, 1, 1049-001 Lisboa, Portugal
{cjs,rita,antonio}@isr.ist.utl.pt

Abstract: The paper addresses the problem of path-following for autonomous underwater vehicles by taking into account the future reference path characteristics, as seen from the vehicle. The methodology used to solve the path-following control problem amounts to posing it as a discrete time path following control problem where a conveniently defined error state space model of the plant is augmented with reference preview data. A piecewise affine parameter-dependent model representation is used to accurately describe the AUV linearized error dynamics for a pre-defined set of operating regions. For each region, the synthesis problem is stated as a state feedback H_2 control problem for affine parameter-dependent systems and solved using Linear Matrix Inequalities (LMIs). The resulting nonlinear controller is implemented within the scope of gain-scheduled control theory using the D-methodology. Simulation results obtained with the INFANTE AUV nonlinear vertical plane model are presented and discussed.

Keywords: Autonomous Vehicles, Feedforward Control, Control Theory

1. INTRODUCTION

This paper describes a solution to the problem of path-following controller design for autonomous underwater vehicle (AUV) taking into account the future reference path characteristics, as seen from vehicle. An application is made to the control of the vertical plane of the prototype INFANTE AUV, built and operated by the Instituto Superior Técnico of Lisbon, Portugal.

Preview control algorithms have been widely used to improve the overall closed loop performance obtained with limited bandwidth feedback compensators when future information on the commands or disturbances is available. A series of papers on application of the Linear Quadratic preview control theory to the design of vehicle active suspensions can be found in the literature. Special emphasis should be given to the pioneering work of Tomizuka Tomizuka (1976), where the optimal preview control problem is formulated and solved, and the impact of different preview lengths on the overall suspension performance is discussed. More recently, Takaba Takaba (2000) addressed the problem of robust servomechanism with preview action mixed LQ/H_∞ design for polytopic uncertain systems using Linear Matrix Inequalities (LMIs).

For linear control systems design, the paper exploits the use of a discrete time state feedback H_2 preview controller synthesis algorithm. In the approach pursued in this paper, results presented in Takaba (2000); Ghaoui and Niculescu (1999) are used to develop the LMI based H_2 preview controller synthesis algorithm for affine parameter-dependent systems.

[1] This work was partially supported by Fundação para a Ciência e a Tecnologia (ISR/IST pluriannual funding) through the POS_Conhecimento Program that includes FEDER funds and by project MAYASub of the AdI. The work of R. Cunha was supported by a PhD Student Grant from the Portuguese FCT POCTI programme.

In the paper, linear state feedback preview controllers are synthesized for a finite number of piecewise affine parameter-dependent discrete time plant models. Each of these models consists of the discrete equivalent of the generalized error linearization for each of the AUV operating regions determined by a well-defined box in the parameter space (vehicle's total speed and angle of attack). The adopted error space is in line with the solutions presented in Cunha and Silvestre (2005); Silvestre (2000) and exhibits high directionality accuracy, by taking into account the current vehicle orientation in the definition of the reference velocities. Related work in the area with applications to helicopters can be found in Paulino et al. (2006a), where the authors apply a similar technique to a rotorcraft terrain-following problem.

The final implementation of the resulting non-linear gain scheduled controller uses the D-methodology described in Kaminer et al. (1995) which guarantees a fundamental linearization property and eliminates the need to feedforward the values of the state variables and inputs at trimming.

The paper is organized as follows. Section 2 introduces a nonlinear model for the vertical plane dynamics of the INFANTE AUV. Section 3 introduces briefly the path-dependent error space used to describe the vehicle dynamics. Section 4 states the preview control problem. Section 5 describes the methodology adopted for H_2 linear controller design where an LMI synthesis technique is applied to affine parameter-dependent systems. Section 6 focuses on the implementation of the nonlinear path-following controller for the INFANTE AUV. Finally, simulation results obtained with the full nonlinear dynamic model are presented in Section 7.

2. VEHICLE DYNAMICS

This section describes the dynamic model of the INFANTE AUV in the vertical plane Silvestre (2000). The vehicle is 4.5 m long, 1.1 m wide and 0.6 m high. It is equipped with two main thrusters (propellers and nozzles) for cruising and fully moving surfaces (rudders, bow planes and stern planes) for vehicle steering and diving in the horizontal and vertical planes, respectively. The notation used and the structure of the

Fig. 1. The INFANTE Vehicle

vehicle model are standard Silvestre (2000); Fossen (1994). The variables u and w denote surge and heave speeds, while θ, q, x, and z denote pitch, pitch rate, x position, and depth, respectively. The symbols δ_b and δ_s represent the bow and stern plane deflections, respectively. With this notation and neglecting the roll stable motion, the dynamics of the AUV in the vertical plane can be written in compact form as

$$m\dot{u} = X_{uu}u^2 + X_{ww}w^2 + X_{qq}q^2 + u^2X_{\delta_b\delta_b}\delta_b^2 + u^2X_{\delta_s\delta_s}\delta_s^2 + X_{\dot{u}}\dot{u} + T, \quad (1)$$

$$\dot{x} = u\cos(\theta) + w\sin(\theta), \quad (2)$$

$$m\dot{w} = muq + (W-B)\cos(\theta) + \frac{\rho}{2}L^2Z_w uw + \frac{\rho}{2}L^3Z_q uq + \frac{\rho}{2}L^2u^2\left[Z_{\delta_b}\delta_b + Z_{\delta_s}\delta_s\right] + \frac{\rho}{2}L^3Z_{\dot{w}}\dot{w} + \frac{\rho}{2}L^4Z_{\dot{q}}\dot{q}, \quad (3)$$

$$\dot{z} = -u\sin(\theta) + w\cos(\theta), \quad (4)$$

$$I_y\dot{q} = z_{CB}B\sin(\theta) + \frac{\rho}{2}L^3M_w uw + \frac{\rho}{2}L^4M_q uq + \frac{\rho}{2}L^3u^2[M_{\delta_b}\delta_b + M_{\delta_s}\delta_s] + \frac{\rho}{2}L^4M_{\dot{w}}\dot{w} + \frac{\rho}{2}L^5M_{\dot{q}}\dot{q}, \quad (5)$$

$$\dot{\theta} = q, \quad (6)$$

where equations (1), (3), and (5) describe the surge, heave, and pitch motion, respectively, $X_{(.)}$, $Z_{(.)}$, and $M_{(.)}$ are hydrodynamic derivative terms, and z_{CB} represents the metacentric distance. Equations (2), (4), and (6) capture the vehicle kinematics. See Silvestre (2000) for numerical values of the hydrodynamic parameters. The variables m, L, W, B, and I_y are the vehicle's mass, length, weight, buoyancy, and moment of inertia about the y axis, respectively and ρ is the density of the water.

3. ERROR SPACE

The problem of steering the vehicle along a predefined path, which ultimately allows for definition of a bottom-following controller, can be converted into a regulation problem by expressing the state of the vehicle in a conveniently defined error space. This definition requires the introduction of two coordinate systems: the Serret-Frenet frame, $\{T\}$, with origin at the point on the path closest to the vehicle and coordinate axes corresponding to the tangent and normal vectors defined at that point; and the desired body reference frame, $\{C\}$, determined as if the vehicle were following the path with zero error, see Fig. 2. Notice that $\{C\}$ is highly dependent on the vehicle dynamics. However, as will be seen later, $\{C\}$ will never have to be computed explicitly. A reference for the tangent velocity is also required, with $\mathbf{v}_r = [V_r\ 0]^T$ denoting the desired linear velocity in 2D, expressed in $\{T\}$.

Given these definitions, and simplifying the error space presented in Cunha and Silvestre (2005) for the 2D case, the vector $\mathbf{x}_e = [\mathbf{v}_e\ q_e\ d_T\ \theta_e] \in \mathbb{R}^5$; $\mathbf{v}_e \in \mathbb{R}^2$ and output $\mathbf{y}_e \in \mathbb{R}^2$ can be introduced with

$$\mathbf{x}_e = \begin{bmatrix} \mathbf{v}_e \\ q_e \\ d_T \\ \theta_e \end{bmatrix} = \begin{bmatrix} \mathbf{v} - \mathrm{R}(\gamma_T - \theta)\mathbf{v}_r \\ q - q_C \\ (x - x_C)\sin(\gamma_T) + (z - z_C)\cos(\gamma_T) \\ \theta - \theta_C \end{bmatrix} \quad (7)$$

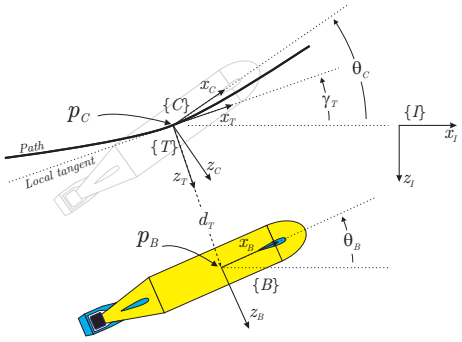

Fig. 2. Coordinate frames: Inertial $\{I\}$; Body $\{B\}$; Serret Frenet $\{T\}$; Desired body $\{C\}$

and $\mathbf{y}_e = \mathbf{v}_e + \mathrm{R}(\gamma_T - \theta)[0\ d_T]^T$, where $\mathbf{v} = [u\ w]^T$, vectors $[x\ z]$ and $[x_C\ z_C]$ are the origins of $\{B\}$ and $\{C\}$ respectively, expressed in $\{I\}$, θ_C is the pitch angle that represents the orientation of $\{C\}$ with respect to $\{I\}$, q_C is the respective time derivative, γ_T is the flight path angle, and $\mathrm{R}(\eta)$ represents the rotation by angle η. It is straightforward to verify that the vehicle follows the path with tangent velocity $\mathbf{v}_r$ and orientation θ_C if and only if $\mathbf{x}_e = 0$.

The output vector $\mathbf{y}_e$ corresponds to a combination of error vector components expressed in the body coordinate system, which is used for tracking purposes. By including $\mathbf{v}_e$ and d_T in $\mathbf{y}_e$, both the velocity and position errors are being considered, with the distance vector expressed in the current body frame.

Assuming that the reference path is a straight line, it satisfies $\dot{V}_r = 0$ and $\dot{q}_C = 0$, and the simplified error dynamics can be written as

$$\begin{cases} \dot{\mathbf{v}}_e &= \dot{\mathbf{v}} - \dot{\mathrm{R}}(-\theta)\mathrm{R}(\gamma_T)\mathbf{v}_r - \mathrm{R}(-\theta)\dfrac{d}{dt}\mathrm{R}(\gamma_T)\mathbf{v}_r \\ \dot{q}_e &= \dot{q} \\ \dot{d}_T &= -u_e \sin(\theta - \gamma_T) + w_e \cos(\theta - \gamma_T) \\ \dot{\theta}_e &= q - \dot{\theta}_C. \end{cases} \tag{8}$$

Notice that at trimming $\frac{d}{dt}\mathrm{R}(\gamma_T)\mathbf{v}_r = 0$ and $q_C = \dot{\theta}_C = 0$. However to account for the preview action these terms are included in the dynamics. Further details on the derivation of the error dynamics can be found in Cunha and Silvestre (2005).

3.1 Error linearization and discretization

For a given straight line path ($q_C = 0$), linear speed V_r, and flight path angle γ_T, define $\mathbf{u}_C$ as the constant input vector that satisfies (1), (3), and (5) at equilibrium ($\dot{u} = 0$, $\dot{w} = 0$, $\dot{q} = 0$), with $\mathbf{v} = \mathrm{R}(\gamma_T - \theta_C)\mathbf{v}_r$, and $\theta = \theta_C$. Then, the linearization of (8) with output vector $\mathbf{y}_e$ about the equilibrium point $\mathbf{x}_e = 0$, $\mathbf{u} = \mathbf{u}_C$ results in

$$\delta\dot{\mathbf{x}}_e = A_e(\zeta)\delta\mathbf{x}_e + B_e(\zeta)\delta\mathbf{u}, \tag{9}$$

$$\delta\mathbf{y}_e = C_e(\zeta)\delta\mathbf{x}_e, \tag{10}$$

where $A_e(\zeta)$, $B_e(\zeta)$, and $C_e(\zeta)$ denote the Jacobians evaluated at the equilibrium condition parameterized by $\zeta = [V_r, \gamma_T]^T$.

The discrete time equivalent of the linear continuous time model (9) is obtained using a zero-order hold on the inputs. Let T be the sampling time and define, with obvious abuse of notation, the augmented discrete time state $\mathbf{x}_d(k) = [\mathbf{x}_e(k)^T, \mathbf{x}_i(k)^T]^T$, where $\mathbf{x}_i(k)$ corresponds to the discrete time integral of $\mathbf{y}_e$. Using this notation, the discrete error dynamics can be written as

$$\mathbf{x}_d(k+1) = A(\zeta)\mathbf{x}_d(k) + B(\zeta)\mathbf{u}(k), \tag{11}$$

where $A(\zeta) = \begin{bmatrix} e^{A_e(\zeta)T} & 0 \\ C_e(\zeta) & I \end{bmatrix}$ and $B = \begin{bmatrix} \int_0^T e^{A_e(\zeta)\tau} d\tau B_e(\zeta) \\ 0 \end{bmatrix}$ for ζ constant.

4. PREVIEW PROBLEM FORMULATION

Better AUV bottom-following performance with limited bandwidth compensators can be achieved by taking into account, in the control law, the seabed characteristics ahead of the AUV obtained from measurements of two echo sounders. The technique used in this paper to develop a tracking controller amounts to augmenting the discrete time error space dynamics with a description of the future seabed evolution as seen by the sensors installed on the AUV.

With the objective of including future path disturbances in the discrete time error space dynamics (11), assume that the AUV moves with constant speed along a given reference path that results from the concatenation of straight lines. A detailed analysis of the error dynamics (8) suggests the introduction of vector

$$\left[-\left(\mathrm{R}(-\theta)\frac{d}{dt}\mathrm{R}(\gamma_T)\mathbf{v}_r \right)^T, 0, 0, -\dot{\theta}_C \right]^T \tag{12}$$

as the perturbation to be previewed. To this effect, and assuming that there is a discontinuity in the reference path resulting from the concatenation of two straight lines that will be crossed by the vehicle at time $t = t_0$, the elements of vector (12) result in

$$\frac{d}{dt}\mathrm{R}(\gamma_T)\mathbf{v}_r = \delta(t - t_0)\left(\mathrm{R}(\gamma_T(t_0^+)) - \mathrm{R}(\gamma_T(t_0^-))\right)\mathbf{v}_r$$

$$\dot{\theta}_C = \delta(t - t_0)\left(\theta_C(t_0^+) - \theta_C(t_0^-)\right)$$

where $\delta(t - t_0)$ is the Dirac's delta function. From (9) the resulting linear error dynamics can be written as

$$\delta\dot{\mathbf{x}}_e = A_e(\zeta)\delta\mathbf{x}_e + B_e(\zeta)\delta\mathbf{u} + W(\zeta)\delta\mathbf{w}, \tag{13}$$

with injection matrix $W(\zeta) = -\begin{bmatrix} \mathrm{R}(-\theta_C) & \mathbf{0}_{2\times 1} \\ \mathbf{0}_{1\times 2} & 0 \\ \mathbf{0}_{1\times 2} & 1 \end{bmatrix}$. Using this interpretation, the seabed disturbance signal, as seen from the AUV, can be modeled as $\mathbf{s}(t) = \sum_i \mathbf{s}(t_i)\delta(t - t_i)$, where $\mathbf{s}(t_i)$ represents an intensity vector, and t_i corresponds to the *ith* concatenation

point crossing time. The corresponding discretization is given by

$$\mathbf{x}_d(k+1) = A(\zeta)\mathbf{x}_d(k) + B(\zeta)\mathbf{u}(k) + B_1(\zeta)\mathbf{s}(k), \tag{14}$$

where $B_1(\zeta) = [(e^{A_e(\zeta)T}W(\zeta))^T, 0]^T$ is obtained from the impulse invariant discrete equivalent of the injection matrix $W(\zeta)$. It is assumed that the sampling period is sufficiently small to consider the reference path changes synchronized with the sampling time. Once again, with obvious abuse of notation, $\mathbf{s}(k) \in \mathbb{R}^s$ corresponds to

$$\mathbf{s}(k) = \begin{bmatrix} \left(\mathrm{R}(\gamma_T(t_k^+)) - \mathrm{R}(\gamma_T(t_k^-))\right)\mathbf{v}_r \\ \theta_C(t_k^+) - \theta_C(t_k^-) \end{bmatrix}.$$

Assuming a preview length of p samples, let $\mathbf{x}_s(k) = [\mathbf{s}(k)^T, \mathbf{s}(k+1)^T, ..., \mathbf{s}(k+p)^T]^T \in \mathbb{R}^{(s(p+1))\times 1}$ be the vector containing all the preview inputs at instant k. The discrete time dynamics of vector $\mathbf{x}_s(k)$ can be modeled as a FIFO queue, given by

$$\mathbf{x}_s(k+1) = D\mathbf{x}_s(k) + B_s\mathbf{s}(k+p+1), \tag{15}$$

where

$$D = \begin{bmatrix} 0 & I & 0 & \cdots & 0 \\ 0 & 0 & I & \cdots & 0 \\ \vdots & \vdots & \ddots & \ddots & \vdots \\ 0 & 0 & 0 & \ddots & I \\ 0 & 0 & 0 & \cdots & 0 \end{bmatrix}, \quad B_s = \begin{bmatrix} 0 \\ 0 \\ \vdots \\ I \end{bmatrix}.$$

Combining the dynamic representation of the seabed (15) with (14) yields the augmented system

$$\mathbf{x}(k+1) = \bar{A}\mathbf{x}(k) + \bar{B}_s\mathbf{s}(k) + \bar{B}\mathbf{u}(k), \tag{16}$$

where

$$\mathbf{x}(k) = \begin{bmatrix} \mathbf{x}_d(k) \\ \mathbf{x}_s(k) \end{bmatrix}, \bar{A} = \begin{bmatrix} A & H \\ 0 & D \end{bmatrix}, \bar{B}_s = \begin{bmatrix} 0 \\ B_s \end{bmatrix}, \bar{B} = \begin{bmatrix} B \\ 0 \end{bmatrix},$$

and $H = [B_1, 0, 0, \cdots, 0]$ represents the injection matrix of the preview signals into the error dynamics. Notice that the D matrix is stable and therefore the augmented system (16) preserves the stabilizability and detectability properties of the original plant.

With the present technique, the preview information is retrieved at p points selected along the path, equally spaced by the distance $d_p = V_t(k)T$. The scalar $V_t(k)$ corresponds to the norm of the projection of the vehicle's velocity vector $\mathbf{v}$ on the path, computed at instant k, which can be obtained from $V_t = [1\ 0]\mathrm{R}(\theta - \gamma_T)\mathbf{v}$. This fact turns out to be of utmost importance, since it allows to naturally redefine the controller visibility distance as a function of the vehicle's speed, preserving the size of the preview input vector.

5. DISCRETE TIME CONTROLLER DESIGN

This section briefly presents a solution to the problem of discrete time state feedback H_2 preview control for affine parameter-dependent systems. In the approach pursued in this paper, results presented in Ghaoui and Niculescu (1999); Takaba (2000) were used to develop the LMI based controller synthesis algorithm. Much of the work in this area is well rooted in the theory of LMIs, which are steadily becoming a standard tool for advanced control system design. In fact, LMIs provide a powerful formulation framework as well as a versatile design technique for a wide variety of linear control problems. Since solving LMIs is a convex optimization problem for which numerical solvers are now available, an LMI based formulation can be seen as a practical solution for many control problems.

5.1 Theoretical background

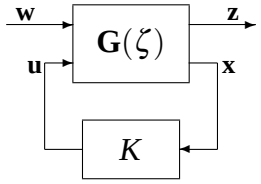

Fig. 3. Feedback interconnection

In what follows, the standard set-up and nomenclature used in Zhou et al. (1995) is adopted, leading to the state-space feedback system represented in Fig. 3. Consider the generalized affine parameter-dependent system $\mathbf{G}(\zeta)$ as a function of the slowly varying parameter vector ζ. It is assumed that ζ is in a compact set $\Theta \subset \mathbb{R}^q$. Suppose that the parameter set Θ can be partitioned into a family of regions that are compact closed subsets Θ_i, $i = 1, \ldots, N$ and cover the desired AUV flight envelope. In the ith parameter region Θ_i, the dynamic behavior of the closed-loop system admits the realization

$$\begin{cases} \mathbf{x}(k+1) = A(\zeta)\mathbf{x}(k) + B_w(\zeta)\mathbf{w}(k) + B(\zeta)\mathbf{u}(k) \\ \mathbf{z}(k) = C_z(\zeta)\mathbf{x}(k) + E(\zeta)\mathbf{u}(k), \ \mathbf{u}(k) = \mathrm{K}\mathbf{x}(k), \end{cases} \tag{17}$$

where $\mathbf{x}(k)$ is the state vector. The symbol $\mathbf{w}(k)$ denotes the input vector of exogenous signals (including commands, disturbances and preview signals), $\mathbf{z}(k)$ is the output vector of errors to be reduced during the controller design process, and $\mathbf{u}(k)$ is the vector of actuation signals. Matrices $A(\zeta)$, $B_w(\zeta)$, $B(\zeta)$, $C_z(\zeta)$, and $E(\zeta)$ are affine functions of the parameter vector $\zeta = [\zeta_1, \ldots, \zeta_q]^T \in \Theta_i$, e.g. $A(\zeta) = A^{(0)} + \zeta_1 A^{(1)} + \ldots + \zeta_q A^{(q)}$. The generalized affine parameter-dependent system $\mathbf{G}(\zeta)$ consists of the plant to be controlled, together with appended weights that shape the exogenous and internal signals and the preview dynamics presented in Section 4.

Given $\mathbf{G}(\zeta)$, an LMI approach for the synthesis of state feedback H_2 controllers for polytopic systems is used to compute $K = [K_d, K_s]$, where K_d and K_s represent the state feedback and feedforward gain matrices respectively, see Ghaoui and Niculescu (1999); Paulino et al. (2006a) for further details.

For augmented discrete time dynamic systems that include large preview intervals $p > 50$, the controller synthesis technique proposed in Ghaoui and Niculescu (1999) leads to LMI optimization problems involving

a large number of variables, which cannot easily be solved using the tools available today. To overcome this limitation, an alternative algorithm for the computation of the feedforward gain matrix is adopted that exploits the particular structure of the augmented preview system, see Paulino et al. (2006a).

6. IMPLEMENTATION

The design and performance evaluation of the overall closed loop system were carried out using the model described in Section 2.

In the application presented here the vehicle is expected to follow a reference path, in the vertical plane, composed by the concatenation of straight lines. During the controller design phase the considered AUV's flight envelope was parameterized by $\zeta = [V_r, \gamma_T]^T$ (equivalently by $[u,w]^T$) and partitioned in 19 regions, see Paulino et al. (2006b). For each operating region, the elements of the discrete time state space matrices were obtained from the linearization of the error dynamics over a dense grid of operating points and then approximated by affine functions of ζ using a Least Squares Fitting. For a relatively dense grid of evaluated operating points, the affine approximation results in a maximum absolute error between entries of the matrices of less than 3% and, an average absolute error of less than 1.4%.

To implement the controller in the scope of gain scheduling control theory, a state feedback gain matrix $\mathrm{K}_i = [\mathrm{K}_{di},\ \mathrm{K}_{si}]$, $i = 1,\ldots,19$ was computed for each of the operating regions using the technique presented in Section 5. During the controller design phase the regions were defined so as to overlap thus avoiding fast switching between controllers. The disturbance input matrix $\bar{B}_w$ was set to $\bar{B}_s$ and the state and control weight matrices $\bar{C}_1$ and $\bar{D}_{12}$, respectively, were set to yield the following performance vector $\mathbf{z}(k) = [\mathbf{z}_1(k)^T\ \mathbf{z}_2(k)^T\ \mathbf{z}_3(k)^T]^T$ where

$$\mathbf{z}_1 = \Big[\sqrt{20}\,u_e, \sqrt{8}\,w_e, \sqrt{0.1}\,q_e, \sqrt{30}\,d_T, \theta_e, x_{i1}, \sqrt{0.1}\,x_{i2}, \sqrt{10}\,x_{i3}\Big]^T$$
$$\mathbf{z}_2 = [W_1(z)\ \delta_b, W_2(z)\ \delta_c]^T,$$
$$\mathbf{z}_3 = \Big[\sqrt{5}\,\delta_b, \sqrt{5}\,\delta_c, \sqrt{0.1}\,T_C\Big]^T$$

and $W_j(z)$, $j = 1,2$ are second order high pass filters implemented by the strictly proper transfer function $W_j(z) = \frac{90(z-0.999)}{(z-1)(z-0.9)}$ that weights the bow and stern control surface signals with the objective of limiting their bandwidth. Furthermore, the third integral state x_{i3} corresponds to discrete time integral action on the bow control surface δ_b which introduces a "washout" to ensure zero bow plane deflection at trimming, see Silvestre (2000).

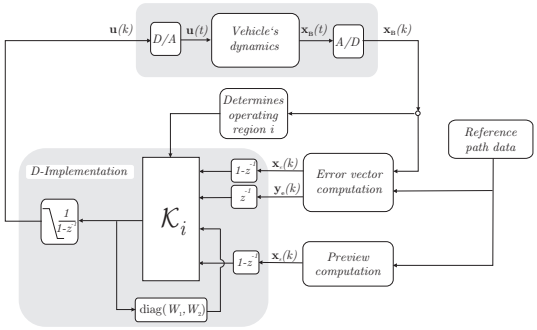

Fig. 4. Implementation setup using gain scheduling and the D-methodology

The final implementation scheme, presented in Fig. 4, was achieved using the D-methodology described in Kaminer et al. (1995). This methodology moves all integrators to the plant input, and adds differentiators where they are needed to preserve the transfer functions and the stability characteristics of the closed loop system. The D-methodology implementation has several important features that are worthwhile emphasizing: i) auto-trimming property - the controller automatically generates adequate trimming values for the actuation signals and for the state variables that are not required to track reference inputs; ii) the implementation of anti-windup schemes is straightforward, due to the placement of the integrators at the plant input. The width of the preview interval suitable for a given vehicle is a compromise between the time-constants associated to the vehicle's dynamics, the computational power available onboard, and the actual sonar range. In the present case, for a maximum vehicle speed of 2.5 m/s, and assuming a sonar range of 50 m provided by a $600\,KHz$ pencil beam sonar, it will be reasonable to consider a preview interval of 15s, to which corresponds a preview length of 150 samples.

7. SIMULATION RESULTS

In this section, a reference path with very sharp transitions is used to evaluate the performance of the nonlinear path-following controller. Fig. 5 shows that,

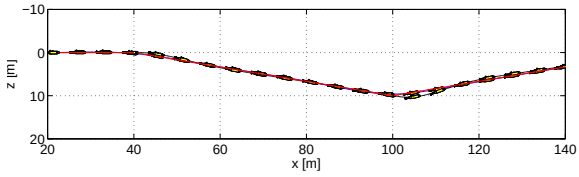

Fig. 5. Trajectories described by the vehicle, with and without preview

for constant slopes, the vehicle trajectory converges to the reference path. It also shows that, the inclusion of preview control action results in a smoother trajectory, largely reducing overshoots and the convergency time. In Fig. 6 a detail including two of the path-following slope transitions shows clearly that the use of preview yields better tracking performance.

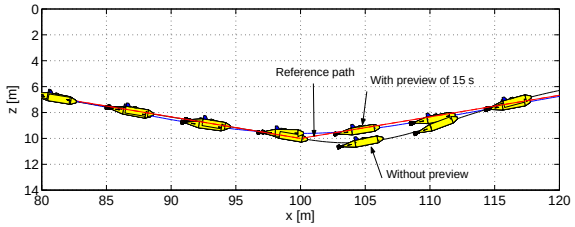

Fig. 6. Detail of the trajectories described by the vehicle, with and without preview. Blow-up of Fig. 5 for $t \in [60, 120]$ s

The time evolution of the error state vectors $\mathbf{x}_e$ without preview and with a preview of 15 **s** experiment is presented in Fig. 7. It can be observed that signal activity, due to the preview action, clearly precedes the path transition points. The actuation signals for the same experiments can be compared in Fig. 8, and it is also clear that, with preview of 15 s, the excursion of the resulting actuation signals is always smaller, and both the state and input variables converge to the trimming faster.

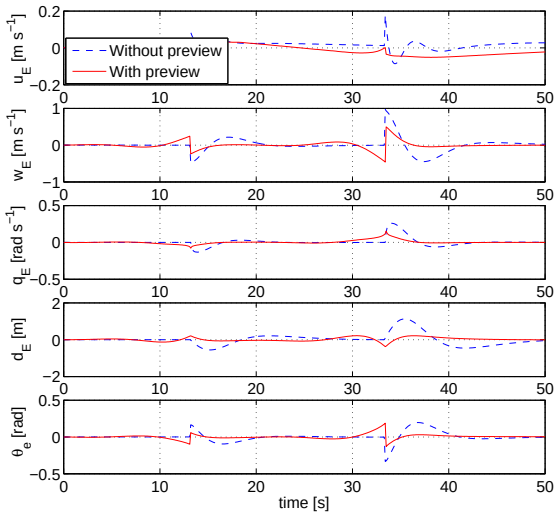

Fig. 7. Time evolution of the error vector $\mathbf{x}_e(t)$, with and without preview

8. CONCLUSIONS

This paper presented the design and performance evaluation of a path-following controller for Autonomous Underwater Vehicles (AUVs).

Resorting to an H_2 controller design methodology for affine parameter-dependent systems, the technique presented exploited an error vector that naturally describes the particular dynamic characteristics of the AUV for a suitable flight envelope.

An alternative algorithm was used for the computation of the feedforward gain matrix that avoids solving Linear Matrix Inequalities involving a large number

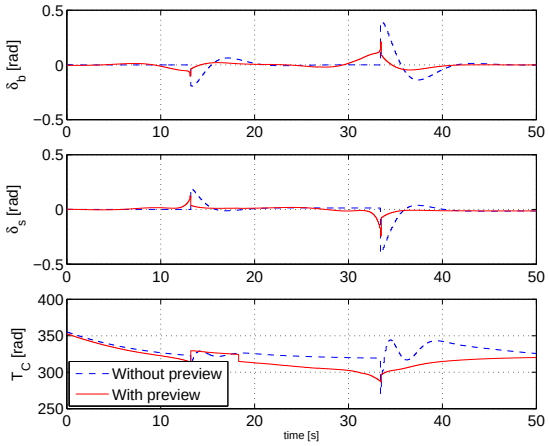

Fig. 8. Time evolution of the actuation $\mathbf{u}(t)$ with and without preview

of unknowns. For a given set of operating regions, a nonlinear controller was synthesized and implemented under the scope of gain-scheduling control theory, using a piecewise affine parameter-dependent model representation.

The effectiveness of the new control laws was assessed in the MATLAB/Simulink simulation environment with a nonlinear model of the INFANTE AUV. The quality of the results obtained clearly indicate that the methodology derived reduces the path following error and simultaneously smooths the actuation signal.

REFERENCES

R. Cunha and C. Silvestre. A 3D Path-Following Velocity-Tracking Controller for Autonomous Vehicles. In *16th IFAC World Congress*, Praha, Czech Republic, July 2005.

T. Fossen. *Guidance and Control of Ocean Vehicles.* John Wiley & Sons, New York, USA, 1994.

L. El Ghaoui and S. I. Niculescu, editors. *Advances in Linear Matrix Inequality Methods in Control*. Society for Industrial and Applied Mathematics, SIAM, Philadelphia, PA, 1999.

I. Kaminer, A. Pascoal, P. Khargonekar, and E. Coleman. A velocity algorithm for the implementation of gain-scheduled controllers. *Automatica*, 31(8):1185–1191, 1995.

Nuno Paulino, Carlos Silvestre, and Rita Cunha. Affine parameter-dependent preview control for rotorcraft terrain following flight. *Accepted for publication AIAA Journal of Guidance, Control, and Dynamics*, 2006a.

Nuno Paulino, Carlos Silvestre, Rita Cunha, and António Pascoal. A Bottom-Following Preview Controller for the INFANTE AUV. Technical report, Institute for Systems and Robotics, ISR-IST, Lisbon, Portugal, 2006b.

C. Silvestre. *Multi-Objective Optimization Theory with Applications to the Integrated Design of Controllers / Plants for Autonomous Vehicles*. PhD thesis, Department of Electrical Engineering, Instituto Superior Técnico, Lisbon, Portugal, 2000.

K. Takaba. Robust servomechanism with preview action for polytopic uncertain systems. *International Journal of Robust Nonlinear Control*, 10:101–111, 2000.

M. Tomizuka. Optimum linear preview control with application to vehicle suspension-revisited. *American Society of Mechanical Engineers - Journal of Dynamic Systems, Measurement, and Control*, 98(3):309–315, 1976.

Kemin Zhou, John C. Doyle, and Keith Glover. *Robust and Optimal Control*. Prentice Hall, Inc., Upper Saddle River, NJ, 1995.